Photonic light-trapping versus Lambertian limits in thin film silicon solar cells with 1D and 2D periodic patterns

Angelo Bozzola,* Marco Liscidini, and Lucio Claudio Andreani

Dipartimento di Fisica "Alessandro Volta", Università degli Studi di Pavia, via Bassi 6, I-27100 Pavia, Italy

*angelo.bozzola@unipv.it

Abstract: We theoretically investigate the light-trapping properties of one- and two-dimensional periodic patterns etched on the front surface of c-Si and a-Si thin film solar cells with a silver back reflector and an anti-reflection coating. For each active material and configuration, absorbance A and short-circuit current density J_{sc} are calculated by means of rigorous coupled wave analysis (RCWA), for different active materials thicknesses in the range of interest of thin film solar cells and in a wide range of geometrical parameters. The results are then compared with Lambertian limits to light-trapping for the case of zero absorption and for the general case of finite absorption in the active material. With a proper optimization, patterns can give substantial absorption enhancement, especially for 2D patterns and for thinner cells. The effects of the photonic patterns on light harvesting are investigated from the optical spectra of the optimized configurations. We focus on the main physical effects of patterning, namely a reduction of reflection losses (better impedance matching conditions), diffraction of light in air or inside the cell, and coupling of incident radiation into quasi-guided optical modes of the structure, which is characteristic of *photonic* light-trapping.

OCIS codes: (040.5350) Photovoltaic; (050.5298) Photonic crystals.

References and links

1. J. Nelson, *The Physics of Solar Cells* (Imperial College Press, London 2003).
2. J. Poortmans and V. Arkhipov (editors), *Thin Film Solar Cells* (Wiley, Chichester, 2006).
3. AM1.5 solar spectrum irradiance data: http://rredc.nrel.gov/solar/spectra/am1.5.
4. E. D. Palik, *Handbook of Optical Constants of Solids* (Academic, Orlando 1985).
5. D. T. Pierce, W. E Spicer, "Electronic structure of amorphous Si from photoemission and optical studies," Phys. Rev. B **5**, 3017–3029 (1972).
6. M. I. Alonso, M. Garriga, C. A. Durante Rincán, E. Hernández, and M. León, "Optical functions of chalcopyrite $CuGa_xIn_{1-x}Se_2$ alloys," Appl. Phys. A **74**, 659–664 (2002).
7. E. Yablonovitch, "Statistical ray optics," J. Opt. Soc. Am. **72**, 899–907 (1982).
8. E. Yablonovitch and G. D. Cody, "Intensity enhancement in textured optical sheets for solar cells," IEEE Trans. Electron. Dev. **29**, 300–305 (1982).
9. M. A. Green, "Lambertian light trapping in textured solar cells and light-emitting diodes: analytical solutions," Progr. Photovolt: Res. Appl. **10**, 235–241 (2002).
10. K. R. Catchpole and A. Polman, "Design principles for particle plasmon enhanced solar cells," Appl. Phys. Lett. **93**, 191113 (2008).

#156735 - $15.00 USD Received 18 Oct 2011; revised 7 Dec 2011; accepted 8 Dec 2011; published 30 Jan 2012

11. K. R. Catchpole and A. Polman, "Plasmonic solar cells," Opt. Express **16**, 21793–21800 (2008).
12. H. A. Atwater and A. Polman, "Plasmonics for improved photovoltaic devices," Nature Mat. **9**, 205–213 (2010).
13. J.N. Munday and H.A. Atwater, "Large integrated absorption enhancement in plasmonic solar cells by combining metallic gratings and antireflection coatings," Nano Lett. **11**, 2195–2201 (2011).
14. J. Krč, M. Zeman, O. Kluth, F. Smole, and M. Topič, "Effect of surface roughness of ZnO:Al films on light scattering in hydrogenated amorphous silicon solar cells," Thin Solid Films **426**, 296–304 (2003).
15. J. Krč, G. Cernivec, A. Campa, J. Malmström, M. Edoff, F. Smole, and M. Topič, "Optical and electrical modeling of Cu(In,Ga)Se_2 solar cells," Optical and Quantum Electronics **38**, 1115–1123 (2006).
16. M. Peters, C. Battaglia, A. G. Aberle, B. Bläsi, J. Luther, and S. Glunz, "*3D optical simulation of scattering in thin film silicon solar cells*," in *Proceedings of the 26th European Photovoltaic Solar Energy Conference and Exhibition*, (Hamburg, September 5-9, 2011) paper 3AV.3.4.
17. M. Agrawal and M. Frei, "Rigorous optical modeling and optimization of thin-film photovoltaic cells with textured transparent conductive oxides," Prog. Photovolt: Res. Appl. DOI: 10.1002/pip.1158 (2011).
18. T. Lanz, B. Ruhstaller, C. Battaglia, and C. Ballif, "Extended light scattering model incorporating coherence for thin-film silicon solar cells," J. Appl. Phys. **110**, 033111 (2011).
19. D. S. Wiersma, "Disordered photonic structures for highly efficient thin film solar cells," OSA Technical Digest (CD) (Optical Society of America, 2010), paper PWA1.
20. M. Steltenpool, J. Rutten, G. van der Hofstad, H. de Groot, J. de Ruijter, A. J. M. van Erven, and G. Rajeswaran, "*Periodic textured TCO for increased light-trapping in thin-film silicon solar cells*," in *Proceedings of the 26th European Photovoltaic Solar Energy Conference and Exhibition* (Hamburg, September 5-9, 2011), paper 3AV.1.55.
21. J. Gjessing, A. S. Sudbø, and E. S. Marstein, "Comparison of periodic light-trapping structures in thin crystalline silicon solar cells," J. Appl. Phys. **110**, 033104 (2011).
22. C. Heine and R. H. Morf, "Submicrometer gratings for solar energy applications," Appl. Opt. **34**, 2476–2482 (1995).
23. S. Hava and M. Auslender, "Design and analysis of low-reflection grating microstructures for a solar energy absorber," Solar Energy Mat. Solar Cells **61**, 143–151 (2000).
24. P. Bermel, C. Luo, L. Zeng, L. C. Kimerling, and J. D. Joannopoulos, "Improving thin-film crystalline silicon solar cell efficiencies with photonic crystals," Opt. Express **15**, 16986–17000 (2007).
25. M. Kroll, S. Fahr, C. Helgert, C. Rockstuhl, F. Lederer, and T. Pertsch, "Employing dielectric diffractive structures in solar cells a numerical study," Phys. Stat. Sol. (a) **205**, 2777–2795 (2008).
26. Y. Lee, C. Huang, J. Chang, and M. Wu, "Enhanced light trapping based on guided mode resonance effect for thin-film silicon solar cells with two filling-factor gratings," Opt. Express **16**, 7969–7975 (2008).
27. D. Zhou and R. Biswas, "Photonic crystal enhanced light-trapping in thin film solar cells," J. Appl. Phys. **103**, 093102 (2008).
28. J. G. Mutitu, S. Shi, C. Chen, T. Creazzo, A. Barnett, C. Honsberg, and D. W. Prather, "Thin film solar cell design based on photonic crystal and diffractive grating structures," Opt. Express **16**, 15238–15248 (2008).
29. R. Dewan and D. Knipp, "Light trapping in thin-film silicon solar cells with integrated diffraction grating," J. Appl. Phys. **106**, 074901 (2009).
30. Y. Park, E. Drouard, O. El Daif, X. Letartre, P. Viktorovitch, A. Fave, A. Kaminski, M. Lemiti, and C. Seassal, "Absorption enhancement using photonic crystals for silicon thin film solar cells," Opt. Express **17**, 14312–14321 (2009).
31. Z. Yu, A. Raman, and S. Fan, "Fundamental limit of light trapping in grating structures," Opt. Express **18**, A367–A380 (2010).
32. Z. Yu, A. Raman, and S. Fan, "Fundamental limit of nanophotonic light trapping in solar cells," Proc. Nat. Ac. Sci. **107**, 17491–17496 (2010).
33. S. Zanotto, M. Liscidini, and L. C. Andreani, "Light trapping regimes in thin-film silicon solar cells with a photonic pattern," Opt. Express **18**, 4260–4274 (2010).
34. C. Ulbrich, M. Peters, B. Bläsi, T. Kirchartz, A. Gerber, and U. Rau, "Enhanced light trapping in thin-film solar cells by a directionally selective filter," Opt. Expr. **18**, A133–A138 (2010).
35. M. Peters, M. Rüdiger, B. Bläsi, and W. Platzer, "Electro optical simulation of diffraction in solar cells," Opt. Expr. **18**, A584–A593 (2010).
36. S. Zanotto, M. Liscidini, and L. C. Andreani, "Efficiency enhancement in thin-film silicon solar cells with a photonic lattice," in *Proceedings of the 25th European Photovoltaic Solar Energy Conference and Exhibition* (Valencia, September 6-10, 2010), paper 1DV.2.66.
37. K. R. Catchpole, "A conceptual model of the diffuse transmittance of lamellar diffraction gratings on solar cells," J. Appl. Phys. **102**, 013102 (2007).
38. K. R. Catchpole and M. A. Green, "A conceptual model of light coupling by pillar diffraction gratings," J. Appl. Phys. **101**, 063105 (2007).
39. R. Esteban, M. Laroche, and J. J. Greffet, "Dielectric gratings for wide-angle, broadband absorption by thin film photovoltaic cells," Appl. Phys. Lett. **97**, 221111 (2010).
40. D. Madzharov, R. Dewan, and D. Knipp, "Influence of front and back grating on light trapping in microcrystalline

#156735 - $15.00 USD Received 18 Oct 2011; revised 7 Dec 2011; accepted 8 Dec 2011; published 30 Jan 2012

thin-film silicon solar cells," Opt. Express **19**, A95–A107 (2009).
41. R. Dewan, I. Vasilev, V. Jovanov, and D. Knipp, "Optical enhancement and losses of pyramid textured thin-film silicon solar cells," J. Appl. Phys **110**, 013101 (2011).
42. A. Mellor, I. Tobs, A. Mart, M. J. Mendes, and A. Luque, "Upper limits to absorption enhancement in thick solar cells using diffraction gratings," Prog. Photovolt: Res. Appl. **19**, 676–687 (2011).
43. N. Senoussaoui, M. Krause, J. Müller, E. Bunte, T. Brammer, and H. Stiebig, "Thin-film solar cells with periodic grating coupler," Thin Solid Films **451-452**, 397–401 (2004).
44. H. Stiebig, N. Senoussaoui, C. Zahren, C. Haase and J. Müller, "Silicon thin-film solar cells with rectangular-shaped grating couplers," Prog. Photovolt: Res. Appl. **14**, 13–24 (2006).
45. L. Zeng, Y. Yi, C. Hong, J. Liu, N. Feng, X. Duan, L. C. Kimerling, and B. A. Alamariu, "Efficiency enhancement in Si solar cells by textured photonic crystal back reflector," Appl. Phys. Lett. **89**, 111111 (2006).
46. L. Zeng, P. Bermel, Y. Yi, B. A. Alamariu, K. A. Broderick, J. Liu, C. Hong, X. Duan, J. D. Joannopoulos, and L. C. Kimerling, "Demonstration of enhanced absorption in thin film Si solar cells with textured photonic crystal back reflector," Appl. Phys. Lett. **93**, 221105 (2008).
47. I. Prieto, B. Galiana, P. A. Postigo, C. Algora, L. J. Martnez, and I. Rey-Stolle, "Enhanced quantum efficiency of Ge solar cells by a two-dimensional photonic crystal nanostructured surface," Appl. Phys. Lett. **94**, 191102 (2009).
48. J. Zhu, Z. Yu, G. F. Burkhard, C. Hsu, S. T. Connor, Y. Xu, Q. Wang, M. McGehee, S. Fan, and Y. Cui, "Optical absorption enhancement in amorphous silicon nanowire and nanocone arrays," Nano Lett. **9**, 279–282 (2009).
49. O. El Daif, E. Drouard, G. Gomard, A. Kaminski, A. Fave, M. Lemiti, S. Ahn, S. Kim, P. Roca i Cabarrocas, H. Jeon, and C. Seassal, "Absorbing one-dimensional planar photonic crystal for amorphous silicon solar cell," Opt. Express **18**, A293–A299 (2010).
50. M. Tsai, H. Han, Y. Tsai, P. Tseng, P. Yu, H. Kuo, C. Shen, J. Shieh, and S. Lin, "Embedded biomimetic nanostructures for enhanced optical absorption in thin-film solar cells," Opt. Express **19**, A757–A762 (2011).
51. Q. Hu, J. Wang, Y. Zhao, and D. Li, "A light-trapping structure based on Bi_2O_3 nano-islands with highly crystallized sputtered silicon for thin-film solar cells," Opt. Express **19**, A20–A27 (2011).
52. A. Naqavi, K. Söderström, F. J. Haug, V. Paeder, T. Scharf, H. P. Herzig, and C. Ballif, "Understanding of photocurrent enhancement in real thin film solar cells: towards optimal one-dimensional gratings," Opt. Express **19**, 128–140 (2011).
53. X. Meng, G. Gomard, O. E. Daif, E. Drouard, R. Orobtchouk, A. Kaminski, A. Fave, M. Lemiti, A. Abramov, P. Roca i Cabarrocas, and C. Seassal, "Absorbing photonic crystals for silicon thin-film solar cells: Design, fabrication and experimental investigation," Solar Energy Mat. Solar Cells **95**, S32–S38 (2011).
54. D. M. Whittaker and I. S. Culshaw, "Scattering-matrix treatment of patterned multilayer photonic structures," Phys. Rev. B **60**, 2610–2618 (1999).
55. M. Liscidini, D. Gerace, L. C. Andreani, and J. E. Sipe, "Scattering-matrix analysis of periodically patterned multilayers with asymmetric unit cells and birefringent media," Phys. Rev. B **77**, 035324 (2008).
56. M. Caglar, S. Ilican, Y. Caglar, and F. Yakuphanoglou, "The effect of Al doping on the optical constants of ZnO thin films prepared by spray pyrolysis method," J. Mater. Sci: Mater. Electron. **19**, 704–708 (2008).
57. Y. Yang, X. W. Sun, B. J. Chen, C. X. Xu, T. P. Chen, C. Q. Sun, B. K. Tay, and Z. Sun, "Refractive indices of textured indium tin oxide and zinc oxide thin films," Thin Solid Films **510**, 95–101 (2006).

1. Introduction

Nowadays, photovoltaic (PV) solar energy and all related research fields are experiencing a very fast growth, in order to develop large-scale solutions for the global energy request. In spite of such a rapid development, the total power delivered by the installed PV modules still covers only a small fraction of electrical energy demand, and this is also due to the relatively high costs of final PV devices. For example, conventional technology for crystalline silicon (c-Si) bulk PV cells [1] requires hundreds of microns of active material, and this, in turn, accounts for up to 40% of the device cost.

In recent years, thin film PV cell technology showed the potential to overcome this problem. In particular, for the materials analyzed in this work, namely c-Si and amorphous silicon (a-Si), thicknesses can be reduced down to a few microns and a few hundreds nanometres, respectively [2], and this could lead to a substantial reduction of PV cell costs.

Unfortunately, the most prominent effect of such a thickness reduction is an absorption reduction, which tends to decrease the photo-generated current. Effects of thickness reduction can be analyzed in short-circuit current density J_{sc}, which is calculated according to assumptions of Sect. 3.1 with the standard AM1.5 incident solar spectrum [3], and reported in Fig. 1 as a

#156735 - $15.00 USD Received 18 Oct 2011; revised 7 Dec 2011; accepted 8 Dec 2011; published 30 Jan 2012

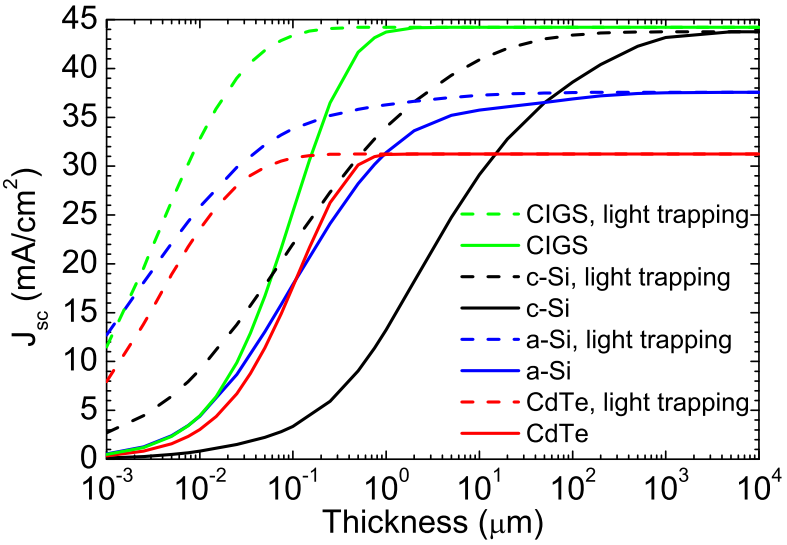

Fig. 1. Short-circuit current density J_{sc} for c-Si (indirect band-gap), a-Si, CdTe and $CuIn_{1-x}Ga_xSe_2$ (CIGS, direct band-gap, taking $x = 0.08$) as a function of thickness, under AM1.5 solar spectrum [3]. Solid lines refer to the single pass case, while dashed lines refer to the Lambertian light-trapping limit denoted as LLα in this paper [9]. In both cases reflection losses are not considered.

function of thickness (solid lines) for a few common PV materials. Optical data for the active materials are taken from Refs. [4] (c-Si, a-Si and CdTe), specifically from [5] for a-Si, and [6] (CIGS).

We observe that direct band-gap semiconductors (like a-Si, CdTe and CIGS) intrinsically require less material to absorb a significant fraction of sunlight with respect to indirect band-gap semiconductors (like c-Si). Indirect band-gap in c-Si is a big disadvantage, since the solar photon flux has its peak in the infrared around 0.8 eV, and a very large fraction of incident photons is lost due to incomplete absorption. To increase absorption and hence the photo-generated current in thin film solar cells, light-trapping must be performed: in other words, incident photons have to enter the device, and their mean dwelling time in the active region must be long enough that, eventually, they are absorbed before escaping the device. Light trapping was first suggested by Yablonovitch and Cody [7, 8], who derived analytical solutions for light path enhancement in *bulk* PV cells with ideal Lambertian light-trapping in the case of very small absorption. These results were then generalized by Green [9], who extended calculations for any degree of absorption in the active material. The effects of Lambertian light-trapping in the latter approach are shown in Fig. 1 for different active materials, as a function of thickness (dashed lines). As it is evident, a proper light-trapping scheme could allow to reduce the active material thickness by an order of magnitude (even more in the case of c-Si), while preserving the same J_{sc} and substantially decreasing the device costs. While related curves are sometimes found in the literature in the large thickness range (see, for example, Fig. 9.16 of Ref. [1] for the case of c-Si), the results of Fig. 1 show that optimal light trapping may be highly beneficial for the efficiency and may have a disruptive effect in terms of cost and material saving for thin- and ultra thin film solar cells.

In recent years, many solutions have been suggested to implement light-trapping schemes in thin film solar cells, ranging from plasmonic metallic structures [10–13] to dielectric structures.

#156735 - $15.00 USD Received 18 Oct 2011; revised 7 Dec 2011; accepted 8 Dec 2011; published 30 Jan 2012

In the latter case, which is also the main focus of this paper, light trapping can be obtained exploiting light scattering by a sub-micron surface roughness (hence a disordered, random structure), as well as adopting photonic crystal patterns (hence an ordered structure), that provides diffraction inside the active material and/or coupling to quasi-guided modes of the structure. The first light trapping scheme is of great interest with polycrystalline active materials, and for PV cells whose front contact is made of a transparent conductive oxide (TCO) with intrinsic surface roughness in the sub-micron range [14–18]. Another approach to light trapping in disordered structures relies on the concept of Anderson localization [19]. The main result is that light scattering can substantially increase the photon dwelling time inside the absorbing material: by proper roughness optimization, the interaction with light can be maximized to increase absorption at low energies, where intrinsic absorption in the active material is weak. While absorption can be increased over a broad spectral range, random structures cannot be engineered easily. The second light-trapping scheme, in which geometrical parameters can be easily varied and the whole structure can be fully engineered, is the one of primary interest for this work. In the Conclusions we will return to the comparison between ordered and disordered light trapping structures, and on their possible merging in an improved PV cell design [20, 21].

Starting from early works on the effect of diffraction gratings [22, 23], PV cells with photonic crystal patterns are extensively studied from both theoretical [24–42] and experimental [43–53] points of view. Silicon is the most commonly studied among the active materials: monocrystalline [45,46], microcrystalline [44], nanocrystalline [51], and, especially, amorphous [43,44,48–50,52] thin film silicon cells with photonic structures have already been fabricated. To obtain an electro-optical characterization of the devices, optical measurements for absorbed, reflected, transmitted, and diffracted power [44,48,49] are generally performed together with external (or internal) quantum efficiency and *I-V curve* measurements [44, 46, 47, 50, 52]. From a theoretical point of view, the effects of photonic patterns are analyzed starting from the Maxwell equations, as both periodicity and PV cell thickness are comparable with wavelength, making traditional ray optics approach unsuitable. Rigorous coupled wave analysis (RCWA) is the most used numerical method to calculate absorption in the active material [24–33, 39, 40], since it directly exploits the periodicity of the structure.

In this work we focus on c-Si and a-Si structures with 1D or 2D square lattice on the front surface (Fig. 2). The holes, whose depth is a variable parameter in the structure, are assumed to be filled with an oxide material, which is also used as an antireflection coating (ARC) on the top surface. The absorbance of the active material and the spectral contributions to J_{sc} are taken as figures of merit and are calculated over the characteristic spectral range of AM1.5 solar spectrum with RCWA. For several thicknesses of active materials in the range of interest for thin film PV cells, the configuration is optimized with respect to the etching depth, the period of the photonic patterns, and the ARC parameters. The calculations are performed over a broader range of active material thickness with respect to the other works in the literature, where typically only one thickness value is investigated. By a detailed investigation of the optical spectra we get insight into the three main physical phenomena involved in light trapping and resulting in absorption enhancement: (**i**) suppression of reflection losses due to better impedance matching, (**ii**) diffraction in air and into the cell material, and (**iii**) coupling with the quasi-guided optical modes supported by the structure, which is often referred to as *photonic light trapping*. As a main goal of this work, results for the optimized structures are compared with Lambertian limits for light-trapping in the ray optics regime. [7–9], which are commonly assumed as reference works in literature for the cases of low and arbitrary absorption, respectively. The rest of this work is structured as follows: in Sec. 2 we present the structures under investigation and in Sec. 3 we deal with the theoretical approach used in this study. The results are presented in Sec. 4, first for c-Si and then for a-Si structures, treating both 1D and square 2D patterns for

#156735 - $15.00 USD Received 18 Oct 2011; revised 7 Dec 2011; accepted 8 Dec 2011; published 30 Jan 2012

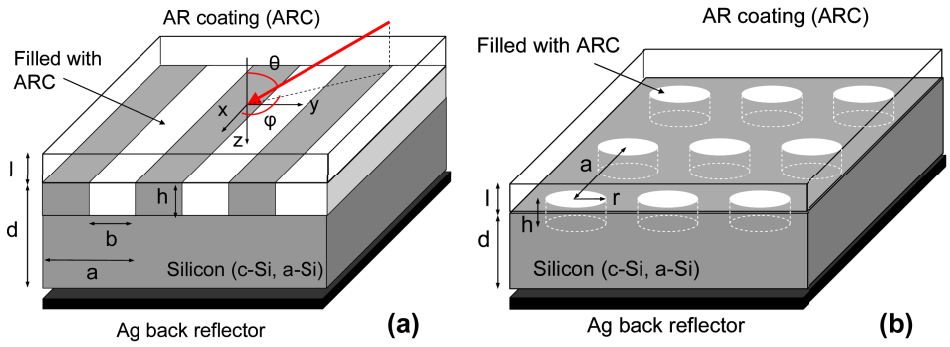

Fig. 2. Scheme of silicon PV cells patterned with a simple 1D photonic lattice (**a**) and with a square 2D lattice (**b**).

each material. Conclusions and prospective developments are summarized in Sec. 5.

2. Analyzed structures

The structures analyzed in this work are PV cells patterned with a 1D or with a square 2D lattice, as shown in Figs. 2(a) and 2(b), respectively. The PV cell surface is taken in the (x,y) plane, with z the direction normal to the cell. The direction of incident radiation is indicated by the red arrow in Fig. 2(a) and can be identified with the pair of polar angle θ and azimuthal angle ϕ. For the present work, we limit ourselves to nearly normal incidence, namely θ=0.1° and ϕ=0° (the choice θ=0.1° is necessary for the convergence of the calculations and it does not substantially modify the results from the normal incidence case, [54]). The results are averaged over the two, orthogonal polarizations. We previously analyzed the dependence of the cell response on the incidence direction and polarization [36], and we found that these structures are rather robust with respect to variations in both θ and ϕ. This is particularly interesting in the case of 1D patterns, since a stronger angular dependence would be expected. Instead, a typical $\cos\theta$ dependence of the current response was found, and the same trend occurs when the polarization direction is parallel (ϕ=0) or orthogonal (ϕ=90 degrees) to the grating [36]. For 2D structures, the angular dependence is expected to be further suppressed, due to higher symmetry and isotropy.

Both 1D and 2D patterns are supposed to be obtained via etching procedure starting from a slab of semiconductor material of thickness d, deposited on a silver (for optical data see Ref. [4]) substrate that serves as back reflector and electric contact. The active materials we consider are c-Si and a-Si, whose optical functions are taken from Ref. [4]. The spectral absorbances of these materials are different, and this affects the typical thickness d required to obtain complete light absorption, making c-Si PV cells much thicker than a-Si ones. Being interested in light-trapping in thin film Si solar cells, we limit the range of thicknesses from 250 nm to 4 μm for c-Si PV cells and from 50 to 500 nm for a-Si PV cells. Especially for the case of a-Si PV cells, the film thickness is limited by diffusion lengths for the photogenerated carriers, which are less than a few hundreds nanometres [2].

For PV cells with 1D pattern, the period is indicated with a, the width of the etched region with b, and the etching depth with h. The grooves are supposed to be filled with a transparent dielectric medium with refractive index n_{ARC}=1.65, and the same dielectric is supposed to be

#156735 - $15.00 USD Received 18 Oct 2011; revised 7 Dec 2011; accepted 8 Dec 2011; published 30 Jan 2012

deposited until a covering slab of thickness l is formed. This layer acts both as a passivating structure for the etched layer as well as an anti-reflection coating (ARC). The value for n_{ARC} is in between that of fused silica (SiO_2, see Ref. [4] for optical data) and that of transparent conductive oxides, as, for example, Al-doped zinc oxide (AZO, see Ref. [56]) and indium tin oxide (ITO, see Ref. [57]). In this way our results are generally applicable without strong variations to PV cells whose patterned layers have very different transport properties, from passivating window layers (for example with SiO_2, as we used in our previous work [33,36]) to conductive layers for carriers extraction. In this work we choose an idealized, dispersion-less, covering dielectric, but more realistic and absorbing materials could be considered without major changes to the conclusions. The thickness of the covering slab l is set to 70 nm for all the investigated structures: this value has been optimized in a previous work on 1D lattices [33], and we have verified that the same optimized value is found for the 2D lattices considered in this work.

For PV cells with a 2D square pattern (Fig. 2(b)), the same notation is used for the lattice period, the ARC thickness, and the etching depth. In this case we consider a 2D lattice of circular rods of radius r etched in the Si slab, and the materials filling fractions are

$$FF_{Si} = 1 - \frac{\pi r^2}{a^2} \quad FF_{ARC} = \frac{\pi r^2}{a^2}. \tag{1}$$

We shall display the results as a function of the ratio r/a (instead of the filling parameters FF), as it gives a more intuitive description of the pattern structure. Attention should be paid to the fact that the ratio b/a for 1D patterns can span the range [0,1], while the ratio r/a is within the range [0,0.5], the upper limit corresponding to rods' contact.

We analyzed also another 2D periodic pattern, namely the triangular lattice of circular rods. We found that best results for triangular pattern are essentially analogous to those for square pattern, as expected from the high symmetry of both lattices. However, rather unexpectedly, the square lattice gives slightly higher short-circuit currents than the triangular lattice. In view of this, in the rest of this paper we present only the results for square patterns.

3. Theory and numerical methods

The electric response of a PV cell is given by its current-to-voltage curve or, more briefly, *I-V curve*. From a theoretical point of view, this relation can be derived assuming an ideal and exponential I-V curve for the p-n junction forming the PV cell and adding a current contribution proportional to the flux of incident photons with energy larger than the band-gap E_g (Ref. [1]). Considering the response of the PV cell unit area rather than that of the whole PV cell, the *J-V curve* can be expressed as:

$$J(V) = J_{sc} - J_0 \left[e^{\frac{eV}{K_B T}} - 1 \right], \tag{2}$$

where J_{sc} is the short-circuit current density, J_0 is the generation current density for the p-n junction, e the electron charge, K_B the Boltzmann constant, and T the thermalized electron temperature of the cell. At a given operating voltage V, the product $V \cdot J(V)$ gives the electrical power converted by PV cell per unit area. It can be shown that this depends nearly linearly upon J_{sc}, and for this reason J_{sc} has been assumed as our main figure of merit. The short-circuit current density J_{sc} is a spectrally-integrated quantity defined as [1]:

$$J_{sc} = e \int_{E_g}^{\infty} A(E) \frac{d\mathcal{N}}{dE} IQE(E) dE \equiv$$
$$e \int_{E_g}^{\infty} A(E) \frac{d\mathcal{N}}{dE} dE \equiv \int_{E_g}^{\infty} \frac{dJ_{sc}(E)}{dE} dE, \tag{3}$$

#156735 - $15.00 USD Received 18 Oct 2011; revised 7 Dec 2011; accepted 8 Dec 2011; published 30 Jan 2012

where $A(E)$ is the absorbance of the active material, $\frac{d_s\mathcal{N}}{dE}$ is the incident solar photon flux (which has dimension of number of incident photons per unit time, per unit surface area, and per unit energy bandwidth), and IQE is the internal quantum efficiency for separation and collection of the photogenerated electron-hole pairs. Since in this work we are concerned with the optical rather than transport properties of the cell, IQE has been set equal to one. In this way one can define the *spectral contribution* dJ_{sc}/dE to the short-circuit current density (Eq. (3)). This in turn is proportional to the absorbance $A(E)$ of the active material in the PV cell, which is taken as our second figure of merit. The integration range has a lower limit 1.12 eV for c-Si, or 1.25 eV for a-Si (the bandgap of a-Si with the data of Ref. [5]). The upper limit is taken to be 3.5 eV in both cases, as the photon flux above this energy is small in the standard AM1.5 solar spectrum [3]. Finally, as in our previous work [33], a black-body dependence is assumed for the photon flux $\frac{d_s\mathcal{N}}{dE}$, with characteristic emission temperature of 5800 K and total irradiance of 100 mW/cm^2, which is that of the AM1.5 solar spectrum. Both the truncation of the integration range and the choice of a blackbody spectrum affect the final results, giving lower J_{sc} with respect to the full AM1.5 solar spectrum, which is slightly richer in photons in the visible range. This is the reason why the subsequent results for Lambertian limits are slightly smaller than those given in Fig. 1: this choice allows to considerably reduce computing time when optimizing the structures. Of course, a real solar cell should be simulated with the full AM1.5 spectrum.

The absorbance $A(E)$ of the active layer and hence J_{sc} are calculated adopting a rigorous electromagnetic approach, starting from Maxwell equations for fields $E(x,y,z)$ and $H(x,y,z)$, and then calculating the scattering matrix S for the configuration under investigation [54, 55]. The PV structure is treated as a multilayer along z (see Fig. 3(a)), with the light incident from the left, under the form of a plane wave. Following the notations of Refs. [33] and [54], and denoting in-plane coordinates $(x,y) \equiv \rho$, the electric field E can be expressed in each point as a Fourier series:

$$E(\rho,z) = \sum_{n=0}^{NPW-1} \tilde{E}(G_n,z) e^{i(k_{//}+G_n)\cdot\rho}, \tag{4}$$

where NPW is the total number of plane waves considered in the simulation, G_n are the reciprocal lattice vectors (taking $G_0 = 0$), and $k_{//}$ is the component of incident wave vector in the (x,y) plane. The Fourier amplitudes $\tilde{E}(G_n,z)$ are obtained solving Maxwell equations in each layer by matrix diagonalization, and then propagating along the structure with proper boundary conditions, with the basis set of plane waves determined by NPW (z dependence is implicitly taken into account, with both propagating and exponentially decaying waves being considered).

Due to translational invariance, we can limit ourselves to the unit cell in the (x,y) plane, and apply Poynting theorem to the volume element enclosed by dashed line in Fig. 3(a). Absorption in the active material is calculated from difference in Poynting vector fluxes across the facets normal to z direction, while any contributions from the other facets vanish due to translational invariance. Normalizing incident power density to unit, energetic balance implies:

$$A + R + T + \sum_{n\neq 0} R_n + \sum_{n\neq 0} T_n = 1, \tag{5}$$

where A is the absorbance of the active material, $R = R_{n=0}$ is the zeroth-order reflectance, and $T = T_{n=0}$ is the zeroth-order transmittance to the Ag substrate. The first sum represents all the power contributions deriving from diffraction in air, and the second sum refers to diffraction in the Ag substrate. In the case of a planar cell, the last two sums in Eq. (5) are absent, due to translational invariance, and thus R and T are the only optical losses (Eq. (5) simply reduces to $A+R+T$=1).

#156735 - $15.00 USD Received 18 Oct 2011; revised 7 Dec 2011; accepted 8 Dec 2011; published 30 Jan 2012

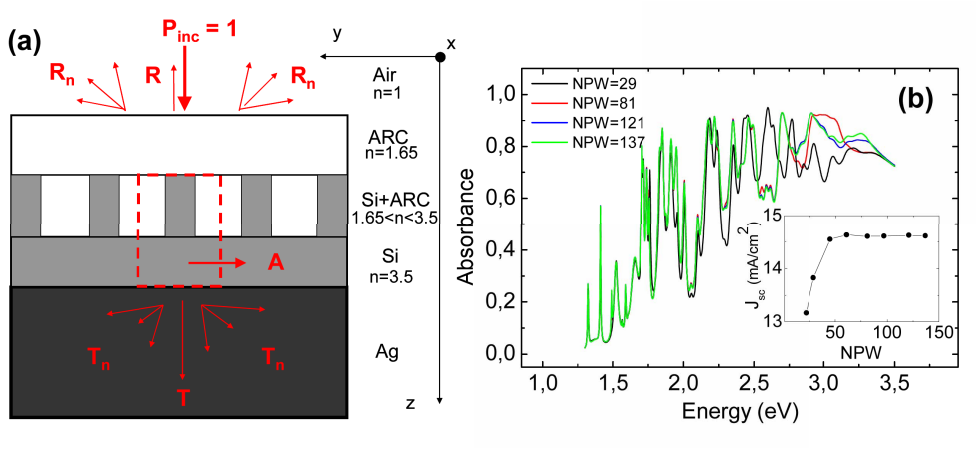

Fig. 3. **(a)** Multilayer subdivision of PV cells along z (the unit cell volume used for A calculation is enclosed with dash line). **(b)** Convergence of the calculated absorbance (main panel) and J_{sc} (inset) as a function of the number NPW of plane waves involved in the calculation.

Note that only the absorption A in the active material contributes to the short-circuit current density, thus the photonic pattern has to increase the absorbance with respect to planar cells without introducing additional losses.

In the limit $NPW \to \infty$, this analysis is exact. In practice, one has to truncate the sum in Eq. (4) to a certain number of plane waves. As the computational time for a large number of plane waves is proportional to NPW^3 because of matrix diagonalization, it is important to choose the NPW that guarantees the convergence of the results in a reasonable computing time. In this respect, symmetry properties of the pattern play a major role, determining both the appropriate number NPW and coupling between incident field and optical quasi-guided modes of the PV structure.

The effect of increasing NPW is shown in Fig. 3(b), where a typical absorbance spectrum is reported for a c-Si PV cell (d=500 nm) with 2D square pattern. The same spectrum is calculated with four different values for NPW. All spectra have similar features at low energy, but noticeable differences are evident with increasing energy. This is because low energy photons can couple only with few modes of the structure, namely the lowest energy modes, and a relatively small NPW is sufficient to reach convergence. On the contrary, high energy photons can couple with more modes, and thus a higher NPW is needed to take into account all accessible modes and to reach convergence. We studied convergence for 2D structures with different pattern configurations, and we concluded that differences between NPW equal to 121 and 137 are small and located at energies above 3 eV, where the solar photon flux is weaker, so NPW=121 is sufficient to full convergence within the whole investigated range. For 1D cells the computation is much shorter, and NPW= 25 is enough to reach full convergence.

In addition, we studied the convergence of the short-circuit current density, which is shown in the inset of Fig. 3(b) for the structure of the main panel of Fig. 3(b) as a function of NPW. For a low NPW, J_{sc} is below the convergence value, then it increases with NPW, showing small oscillations around the convergence value. Even if there is convergence in the spectra only at low energies, the variations around the convergence spectrum are limited to high-energy, where solar photon flux is lower, and they tend to balance in the integration, giving a faster global convergence as compared to absorption spectra.

#156735 - $15.00 USD Received 18 Oct 2011; revised 7 Dec 2011; accepted 8 Dec 2011; published 30 Jan 2012

We compared our results with Lambertian limits to light trapping in *bulk* PV cells. The upper limits for the enhancement of light path inside the active material were first derived under three assumptions [7, 8]:

- The structure has a front Lambertian scatterer or a back Lambertian reflector on the bottom. In both cases transmitted or reflected light is randomized with isotropic angular distribution at every energy. Furthermore, intrinsic reflection losses of the active material are set to zero, and an ideal back reflector is located at the bottom.

- The intrinsic absorption of the active material is sufficiently low for both the *single-pass* and the *enhanced* absorbance. This situation is referred to as *weak absorption regime* and is described by the condition:
$$4n^2\alpha d \ll 1, \tag{6}$$
where n is the real part of the refractive index, α is the absorption coefficient, and d the thickness of the active material.

- The film thickness d is much larger than wavelength λ/n inside the active material, and this makes ray optics arguments suitable.

The absorption can thus be described and quantified in terms of the product $\alpha(E)d_{\text{eff}}$, with d_{eff} being the effective light path inside the active material in a given configuration. For example, if we consider a single-pass through a planar slab, neglecting reflection losses, the product αd_{eff} has a direct interpretation, as the total absorbance A_{sp} is:

$$A_{sp}(E) = 1 - e^{-\alpha(E)d}. \tag{7}$$

Under Yablonovitch hypothesis, it can be shown using ray optics or statistical mechanics arguments that the maximum light path is enhanced by a factor $4n^2/\sin^2\gamma$, with γ half of the apex angle of the cone subtended by the dielectric medium surrounding the cell. In the case of a planar cell surrounded by an isotropic medium ($\sin\gamma$=1), the maximum enhancement is given by $4n^2$, which corresponds to nearly 50 for silicon near the band gap and gives an active material absorbance equal to:

$$A_{LL0}(E) = 1 - e^{-4n^2\alpha(E)d}, \tag{8}$$

where reflection losses are neglected. Along the manuscript, this first Lambertian limit (i.e., weak absorption and neglecting reflection losses) will be denoted by LL0.

More recently, a general limit to Lambertian light-trapping has been derived by Green considering the case of arbitrary absorption and providing an analytic expression for light path enhancement as a function of the photon energy [9]. In this case, assuming $\sin\gamma$=1, it can be shown that the maximum absorption enhancement is lower than in the LL0 limit, as the weak absorption hypothesis is relaxed and the enhancement expected by light trapping is smaller when absorption is larger. We refer to [9] for details of the theoretical treatment. This general Lambertian limit will be denoted by LLα, and it is the most relevant for our work, since active material's absorption is not negligible in most of the investigated configurations. To compare properly with the LL0 limit, we take also the LLα limit in the case of no reflection losses.

Both light trapping limits investigated by Yablonovitch and Green are valid in the limit of ray optics, i.e., they assume that the active material thickness is much larger than the wavelength of light. In the present study, the typical dimensions of thin-film solar cells are comparable to the wavelength of light in most of the spectral range. In the literature this situation is often referred to as *photonic* light-trapping, in contrast with the case of *bulk* PV cells. Light trapping in the (nano)photonic regime has been investigated in Refs. [31, 32] for the case of weak absorption,

#156735 - $15.00 USD Received 18 Oct 2011; revised 7 Dec 2011; accepted 8 Dec 2011; published 30 Jan 2012

where it is shown that the LL0 limit can be overcome in some circumstances. Still, the general limit to light trapping for any material thickness and for arbitrary absorption is unknown. Here we shall take the LL0 and LLα limits as references for the calculated short-circuit current and absorbance spectra, since they can be easily calculated and provide a continuous transition to the case of thick cells, where the ray optics treatment is rigorously valid. In fact, the dashed curves of Fig. 1 are calculated for the realistic case of the LLα limit.

In the case of *photonic* light-trapping, it is difficult to introduce an effective light path. Thus we define an absorption enhancement factor F with respect to the single pass absorption A_{sp} as

$$F(E) = \frac{A(E)}{A_{sp}(E)} = \frac{A(E)}{1 - e^{-\alpha(E)d}}, \tag{9}$$

where $A(E)$ is the structure absorption, which can be calculated analytically or numerically depending on the cell geometry. It is worth noticing that the two limits discussed above can be described using Eq. (9). In particular, in the case of weak absorption the expression gives back the typical $4n^2$ enhancement factor, which can be considered as a reference value for Lambertian light trapping. As it will be evident from the results in the next section, reaching Lambertian light-trapping limits over a broad spectral range is a very difficult task, which can be partly (but not fully) achieved with the periodic structures considered in this work.

4. Results and discussion

We analyze separately the properties of c-Si and a-Si PV cells patterned with photonic lattices. 1D and square 2D patterns are compared for several thicknesses d in range of interest for thin film solar cells, according to observations of Sect. 2. For brevity, only one thickness is analyzed in detail for each active material (1 μm for c-Si and 300 nm for a-Si), and the results for structures of varying thickness are described at the end of each material's subsection.

At a fixed active material thickness d, the analysis is performed in the following way. First, a contour plot of J_{sc} is calculated with the scattering matrix formalism varying at the same time the etching depth h and the ratio b/a (for 1D pattern) or r/a (for square pattern). According to observations of Sec. 3, the number NPW of plane waves is chosen to be 45 for 2D square pattern. Optimal pattern configurations are then identified from maxima in the contour plot, and the corresponding spectra are analyzed in detail. For each optimal configuration, optical spectra for reflectance R, transmittance T, absorbance A, and diffracted power are calculated with a NPW that ensures convergence over the whole spectrum (NPW=25 for 1D patters and 121 for 2D square patterns). Finally, the absorption enhancement F with respect to single pass absorption without reflection losses is compared with the Lambertian limits LL0 and LLα to light-trapping.

Some relevant reference spectra for A and J_{sc} are considered. For absorbance, the comparison is made with the absorbance of a bare slab of active material, without ARC or back reflector and considering the cases with and without reflection losses. This comparison is useful because it directly recalls intrinsic properties of the active material in terms of bare absorption and reflection. The energy range for calculations can thus be subdivided into two ranges: one at low energy, where patterning enhances absorption due to light-trapping, and the other one at high energy, where total absorption occurs even without light-trapping, and, actually, reflection and diffraction in air have to be minimized.

For short-circuit current density J_{sc} and spectral contributions dJ_{sc}/dE, the comparison is made with a reference cell with same thickness d of the investigated configuration, planar geometry, Ag back reflector, and single-layer ARC on top. Optical spectra for reference cells are calculated following the same procedure used for patterned cells. The parameters of the ARC

#156735 - $15.00 USD Received 18 Oct 2011; revised 7 Dec 2011; accepted 8 Dec 2011; published 30 Jan 2012

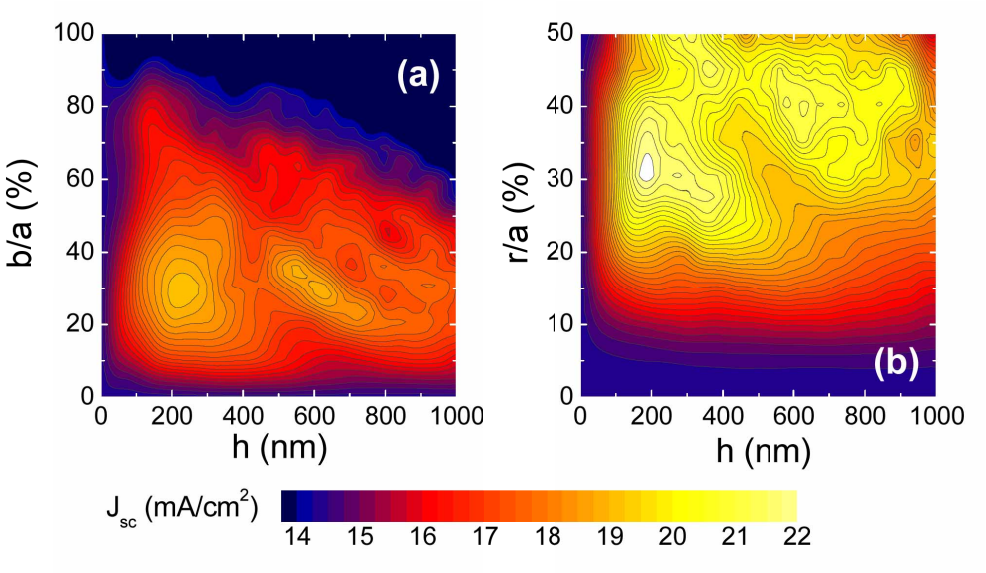

Fig. 4. Contour plot of short-circuit current density J_{sc} as a function of etching depth h and ratios b/a and r/a (in %) for c-Si PV cells patterned with a simple 1D lattice (**a**) and square 2D lattice (**b**). For both patterns the thickness d=1μm and the optimal period a=600 nm.

are optimized to give the highest possible J_{sc} from the reference cell. To make a proper comparison, optimizations (like random texturing) that are common in commercial cells are not considered here.

4.1. Crystalline silicon (c-Si)

The contour plots for the short-circuit current density J_{sc} for c-Si PV cells of thickness d=1 μm patterned with simple 1D and square 2D lattices are shown in Figs. 4(a) and 4(b). One can immediately note that the 2D square pattern is much more performing that the 1D one over a broad range of pattern parameters. Shallow and deep pattern configurations emerge as the maxima in the contour plot. In particular for simple 1D pattern we find:

- **a shallow configuration**, with a=600 nm, h=240 nm, b/a=0.3 and J_{sc}=19.13 mA/cm^2;
- **a deep configuration**, with a=600 nm, h=560 nm, b/a=0.35 and J_{sc}=18.86 mA/cm^2.

For 2D square pattern we find:

- **a shallow configuration**, with a=600 nm, h=190 nm, r/a=0.33 and J_{sc}=22 mA/cm^2;
- **a deep configuration**, with a=600 nm, h=595 nm, r/a=0.42 and J_{sc}=21.3 mA/cm^2.

As we can see, contour plots are smooth over the whole investigated range of parameters, with several local maxima. There is also a good tolerance in J_{sc} around the optimal configuration with respect to variations in h and b/a, or r/a: J_{sc} decreases no more than 2% upon relative variations of $\pm$10% around the optimal values.

Optical spectra for the optimized structures with simple 1D and 2D square patterns are shown in Fig. 5. Starting from reflectance and diffraction in air (Figs. 5(a) and 5(d)), we observe a gradual decrease of these quantities from reference planar cells to 1D and then 2D patterned

#156735 - $15.00 USD Received 18 Oct 2011; revised 7 Dec 2011; accepted 8 Dec 2011; published 30 Jan 2012

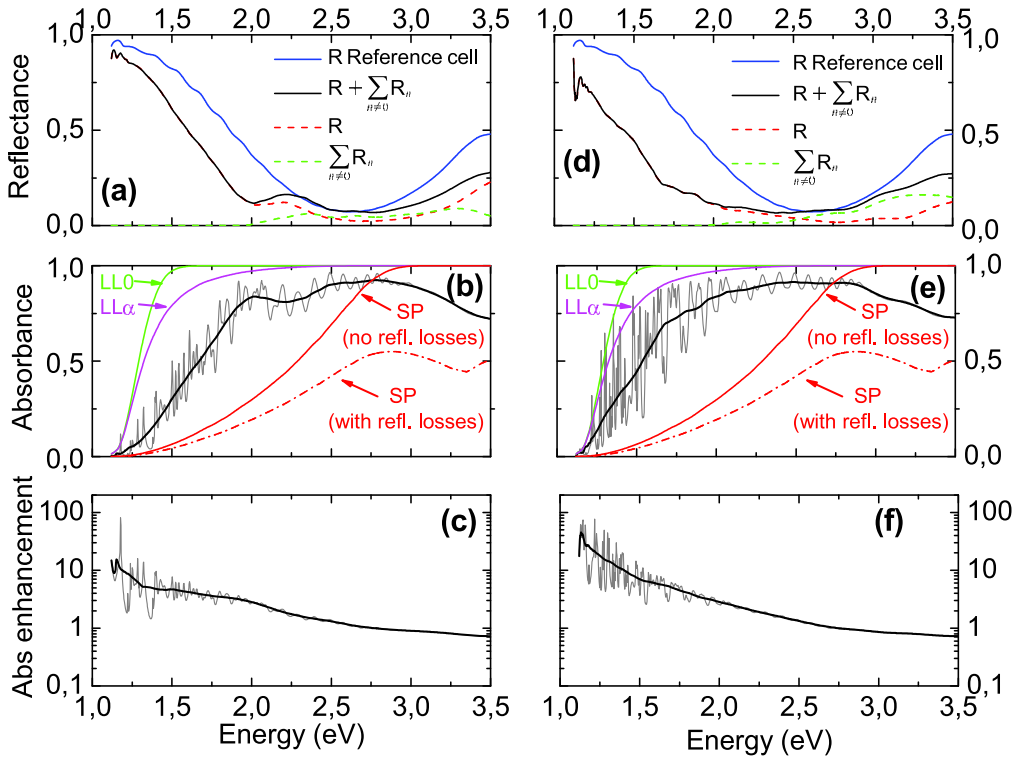

Fig. 5. Calculated optical spectra (for unpolarized light) for c-Si PV cells patterned with optimal 1D simple lattice (d=1 μm, a=600 nm, h=240 nm, b/a=0.3): reflectance $R_{n=0}$ and contributions from diffraction in air $\sum_{n\neq 0} R_n$ (**a**), absorbance A (**b**) and absorption enhancement F (**c**). Calculated optical spectra (for unpolarized light) for c-Si PV cells patterned with optimal 2D square lattice (d=1 μm, a=600 nm, h=190 nm, r/a=0.33): reflectance $R_{n=0}$ and contributions from diffraction in air $\sum_{n\neq 0} R_n$ (**d**), absorbance A (**e**) and absorption enhancement F (**f**). For absorbance the Lambertian limits LL0 and LLα are reported, together with single pass (SP) absorption with and without reflection losses. The thin grey lines refer to the calculated data, while the thick black lines are the corresponding smoothed quantities.

cells. For the patterned cell, the contribution $\sum_{n\neq 0} R_n$ is present, but the total reflectance, which includes all diffraction orders, is always lower than the reflectance R of the reference cell; a similar trend is observed as for the zero-order reflectance.

This is due to both the better impedance matching condition (because the patterned layer has an intermediate effective refractive index) and to light trapping. At low energies, incomplete absorption gives the dominant R contribution, that is nearly complementary to absorbance spectrum. At high energies there is a residual reflection, but it is evident that the intermediate patterns provides a spectral band of low reflectance, which is broader than that of the reference cell with single-layer ARC. Diffraction in air is a substantially small and constant term in 1D cells, but it is larger in 2D cells, due to the larger number of diffraction modes allowed by symmetry. Diffraction in air can be strongly reduced by decreasing the lattice period, as it will be evident for a-Si cells.

Absorbance spectra have a rich variety of optical features and are shown in Figs. 5(b) and 5(e) for c-Si PV cells with simple 1D and 2D square patterns, respectively. Starting from the

#156735 - $15.00 USD Received 18 Oct 2011; revised 7 Dec 2011; accepted 8 Dec 2011; published 30 Jan 2012

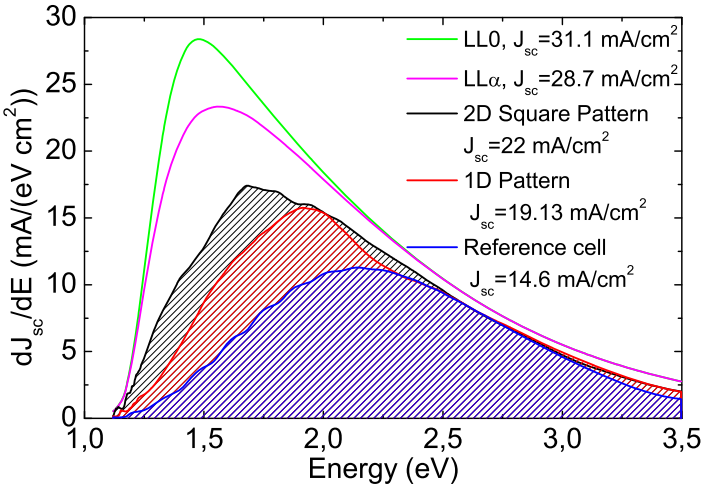

Fig. 6. Spectral contributions dJ_{sc}/dE to short-circuit current density J_{sc} for c-Si PV cells patterned with optimized 1D and square 2D square lattices. Thickness d=1μm, optimal period a=600 nm.

single pass case, we note that a planar slab of thickness d=1 μm has the potential to absorb nearly all incident light with energy greater than 2.75 eV, at least when a proper ARC is applied on the front surface. Light trapping has to be tailored to give its maximum contribution below this energy threshold. This is done optimizing the structures, and best results reported in Figs. 5(b) and 5(e) show several peaks deriving from coupling with quasi-guided modes. Since the typical spectral width of each peak is narrow compared to the useful solar spectrum bandwidth, a collection from multiple peaks deriving from different coupling processes is needed to obtain relevant increase in J_{sc}.

Due to the higher number of quasi-guided modes available related to higher symmetry, 2D patterns are always better than 1D ones. For both patterns, the line shape of the resonance broadens for increasing energy, according to the fact that a higher intrinsic absorption produces lower and broader features in the absorption spectra [31, 32].

For c-Si cells with 1D pattern, the calculated absorbance is always lower than both LL0 and LLα limits. This is evident from absorption enhancement F reported in Fig. 5(c), which reaches a smoothed maximum value of 15, still far away from $4n^2$ maximum value for the LL0 limit in the weak absorption regime. For c-Si PV cells with 2D square lattice, instead, the calculated absorbance can overcome both LL0 and LLα limits, at least at the exact energies for coupling with quasi-guided modes, in agreement with predictions from temporal coupled-mode theory [31, 32]. When absorption enhancement is smoothed, the maximum value reaches 40 to 45 near the c-Si band gap energy, not far away from $4n^2$ for Lambertian limit to light-trapping (Fig. 5(f)).

Smoothed spectral contributions dJ_{sc}/dE to short-circuit current density are shown in Fig. 6. In terms of short-circuit current density, patterning gives a +30% enhancement for the 1D case, and a +55% enhancement for the 2D square case, compared to a reference cell with the same thickness d=1 μm.

In order to check the validity of our optimization procedure, we compared our results with others in literature that are available for the same structures at a few specific thicknesses. For example, Refs. [29, 40] reported results about 1 μm thick microcrystalline Si PV cells with frontal 1D grating and back reflector, with optimal period a=600 nm and optimal grating height

#156735 - $15.00 USD Received 18 Oct 2011; revised 7 Dec 2011; accepted 8 Dec 2011; published 30 Jan 2012

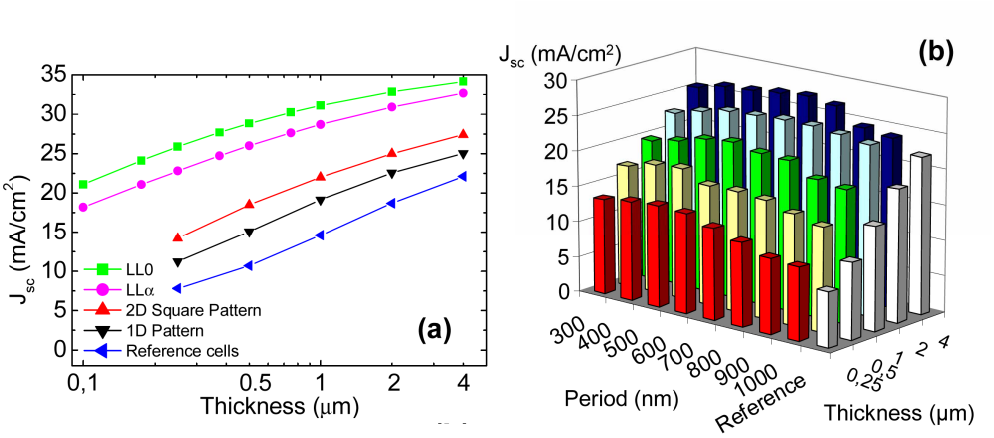

Fig. 7. **(a)** Calculated short-circuit current densities J_{sc} for c-Si PV cells patterned with optimized 1D and square 2D lattices varying the thickness d of the starting active material's slab. **(b)** J_{sc} for optimal configurations as a function of period a and thickness d.

h=200 nm, that are in good agreement with our results.

The results of our simulations for c-Si PV cells are summarized in Fig. 7(a), where short-circuit current densities J_{sc} are shown for the optimal configurations for each different thickness d. Periodic patterns give nearly the same current density gain at every thickness, while J_{sc} strongly decreases in thinner reference cells (as indicated by the blue curve of Fig. 7(a)). This makes light trapping much more relevant for thinner structures. For example, only a +23% increase in J_{sc} is calculated for a 4 μm thick c-Si PV cell with optimized 2D square pattern, but a +82% is obtained with a 250 nm thick cell with the same, properly optimized pattern.

Finally, the dependence of J_{sc} on lattice period is studied, as shown in Fig. 7(b) for the optimized configurations at different d and a in the range from 300 to 1000 nm. Upon variations of a, light trapping can be tuned in order to produce a dense distribution of absorption peaks in the desired spectral region. With a short period, only high energy photons can couple into the structure, and the low energy ones experience the textured layer as uniform and characterized by an effective refractive index intermediate between those of c-Si and ARC. Reflection and diffraction losses can be reduced, but light trapping is limited to high energies, where solar photon flux is weak. Light trapping can be tuned toward low energies by increasing the period a, but also diffraction in air is increased. Optimal periods derive from balance of these two mechanisms: the thicker the cell, the more light-trapping has to be tuned towards lower energies.

This causes the optimal period for thinner structures (d=250 nm) to be around 450 nm, then it increases up to 600 nm for intermediate structures (d=1 μm) and up to 700÷800 nm for thicker structures (d=2 and 4 μm). Nevertheless, it is interesting to observed that the optimal period has a much smaller increase than the cell thickness, and that the short-circuit current has a relatively weak dependence on the lattice period close to the optimal value, being always considerably improved with respect to the reference cell.

4.2. Amorphous silicon (a-Si)

The contour plots of short-circuit current density J_{sc} for a-Si PV cells of thickness d=300 nm patterned with simple 1D and square 2D lattices are shown in Fig. 8(a) and 8(b), respectively. As for c-Si structures, various configurations emerge.

#156735 - $15.00 USD Received 18 Oct 2011; revised 7 Dec 2011; accepted 8 Dec 2011; published 30 Jan 2012

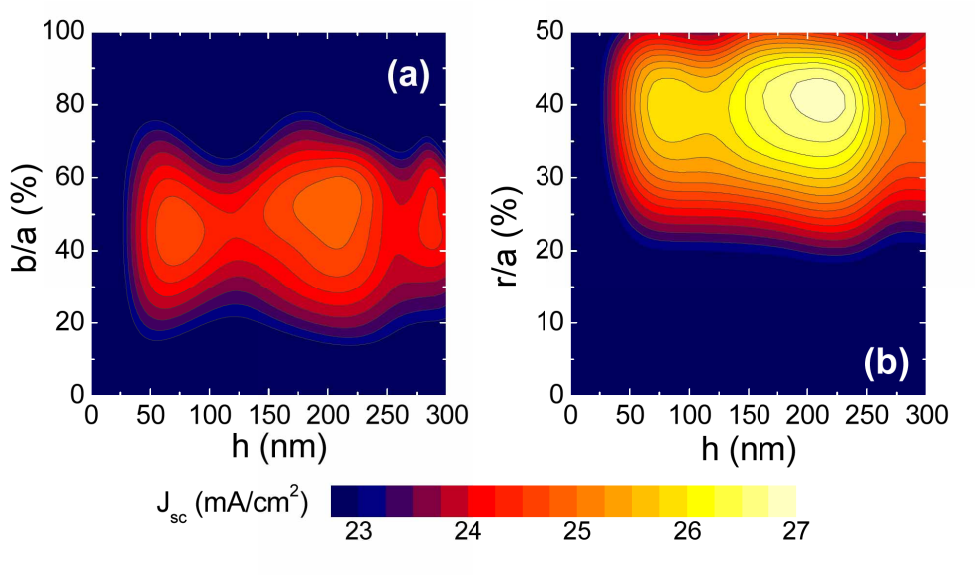

Fig. 8. Contour plot of short-circuit current density J_{sc} as a function of etching depth h and ratios b/a and r/a (in %) for a-Si PV cells patterned with a simple 1D photonic lattice (**a**) and square 2D lattice (**b**). For both patterns the thickness d=300 nm and the optimal period a=300 nm.

For cells with 1D simple pattern we find:

- **a shallow configuration**, with a=300 nm, h=75 nm, b/a=0.45 and J_{sc}=24.7 mA/cm^2;
- **a deep configuration**, with a=300 nm, h=210 nm, b/a=0.55 and J_{sc}=25 mA/cm^2.

For 2D square pattern we find only:

- **a deep configuration**, with a=300nm, h=215 nm, r/a=0.4 and J_{sc}=26.9 mA/cm^2.

Optical spectra for a-Si PV cells with optimized patterns are shown in Fig. 9. Starting from reflectance (Figs. 9(a) and 9(d)), we observe the same trend of c-Si PV cells: $R_{n=0}$ decreases in 1D and, especially, in 2D patterned cells. A spectral band with nearly zero reflection is obtained from 2 to 2.75 eV in 1D cells and up to 3.25 eV in 2D cells. Only two residual contributions are observed: one at high energy ($R_{n=0} \approx 0.1$) and one around E=1.6 eV, which is present in all devices (with just a gradual red shift in the reflection peak from reference to 1D and then 2D cells). Diffraction in air, instead, is substantially suppressed due to the short period a, differently from c-Si cells.

Absorbance spectra are reported in Figs. 9(b) and 9(e), and are basically complementary to reflectance spectra, as for c-Si structures. The main differences between c-Si and a-Si PV cells are due to different spectral absorbances of the active materials. Being the a-Si a direct band gap semiconductor, its absorption coefficient rises more rapidly above the band gap, and this limits the spectral range where light-trapping can be applied only to low energy photons. For example, for the thickness d=300 nm, light trapping can give a contribution only for energies below 2 eV, where absorption is sufficiently weak.

Being this spectral range smaller than that typical of c-Si, the absorption enhancement provided by light trapping gives a less significant relative contribution. In addition, all spectra are

#156735 - $15.00 USD Received 18 Oct 2011; revised 7 Dec 2011; accepted 8 Dec 2011; published 30 Jan 2012

smoother than in c-Si PV cells, and only broad peaks are present since intrinsic absorption is higher than in c-Si. Absorption enhancements F reported in Fig. 9(c) and 9(f) are lower than 10, and still far from $4n^2$ Lambertian limit. This is mainly due to the high intrinsic absorption for the single pass, that gives low F according to Eq. (9): for a-Si, the LLα limit is more relevant in most of the spectral range. 2D square pattern gives higher J_{sc}, with a relative +20% increase. The simple 1D pattern follows with a relative +11% increase in J_{sc} with respect to reference cell.

Results for a-Si structures of thickness d=300 nm are summarized with spectral contributions dJ_{sc}/dE shown in Fig. 10. We compared our results for a-Si structures with those in the literature at a few specific thickness, as we made for c-Si cells. For example, Ref. [25] reported results for a 338 nm thick a-Si PV cell with a 1D front grating (the structure is the same of Fig. 2(a)), characterized by optimal period a=360 nm, etching depth h=80 nm and Si fill fraction $1-b/a$=58%. This is in good agreement with the data in the contour plot of Fig. 8(a): we observe the main maximum at a larger etching depth, but also a secondary maximum having features compatible with the aforementioned work. Also Ref. [30] reported a 100 nm thick a-Si PV cell with frontal 1D grating of optimal period a=450 nm and Si fill fraction $1-b/a$=68%. Also in this case we find good agreement with our results, with optimal period a=500 nm and $1-b/a$=65%.

The effects of photonic light trapping on a-Si structures as a function of thickness d are illustrated in Fig. 11(a). As for c-Si structures, patterned cells have better performance with respect to planar reference ones, with 2D square pattern being better than 1D pattern. In addition, light trapping is more relevant for thinner cells. For example, a +12% J_{sc} increase is calculated for a 500 nm thick cell with optimized 2D square pattern, but a +49% increase is obtained in a 50 nm thick cell with the same, properly optimized pattern.

The differences caused by absorption properties of c-Si and a-Si are evident considering the dependence of optimal J_{sc} on thickness d and period a, as shown in Fig. 11(b). For thin cells (d=50 and 100 nm), optimal a is of the order of 500 nm and a trend similar to c-Si cells is observed. For thicker cells we do not observe this trend, and, actually, for d=300 nm the shortest a is the best one. Taking into account that a longer a is needed to couple low energy photons inside the structure, we conclude that the absorption enhancement provided by a longer a is overcome by additional losses deriving from diffraction in air. The highest J_{sc} is thus obtained with a shorter a, since diffraction in air is largely suppressed, and reduction of reflection losses becomes the key effect determining the absorption enhancement.

5. Conclusions and future developments

We investigated the optical properties of silicon (c-Si and a-Si) PV cells patterned with simple 1D and square 2D photonic lattices on the front surface. Patterns have been studied with rigorous coupled wave analysis and optimized for several thicknesses in the range of interest for thin-film PV cells. We conclude that patterning can give a substantial absorption increase, which contributes towards higher short-circuit current densities J_{sc} and hence higher conversion efficiencies of the PV structures under consideration. For c-Si, relative increase goes from +23% with a 4 μm thick cell, up to +82% with a 250 nm thick cell. For a-Si, instead, J_{sc} relative increase goes from +12% with a 500 nm thick cell, up to +49% with a 50 nm thick cell. These results are rather tolerant with respect to small (up to 10%) deviations from the optimal parameters. Actually, fabrication imperfections might even improve the light trapping performance thanks to the effects of disorder, as discussed below.

The optical properties of the investigated structures are determined by the interplay between different physical effects: **(i)** reflection, **(ii)** diffraction in air and into the cell material, and **(iii)** coupling with the quasi-guided optical modes supported by the structure. The dominance of

#156735 - $15.00 USD Received 18 Oct 2011; revised 7 Dec 2011; accepted 8 Dec 2011; published 30 Jan 2012

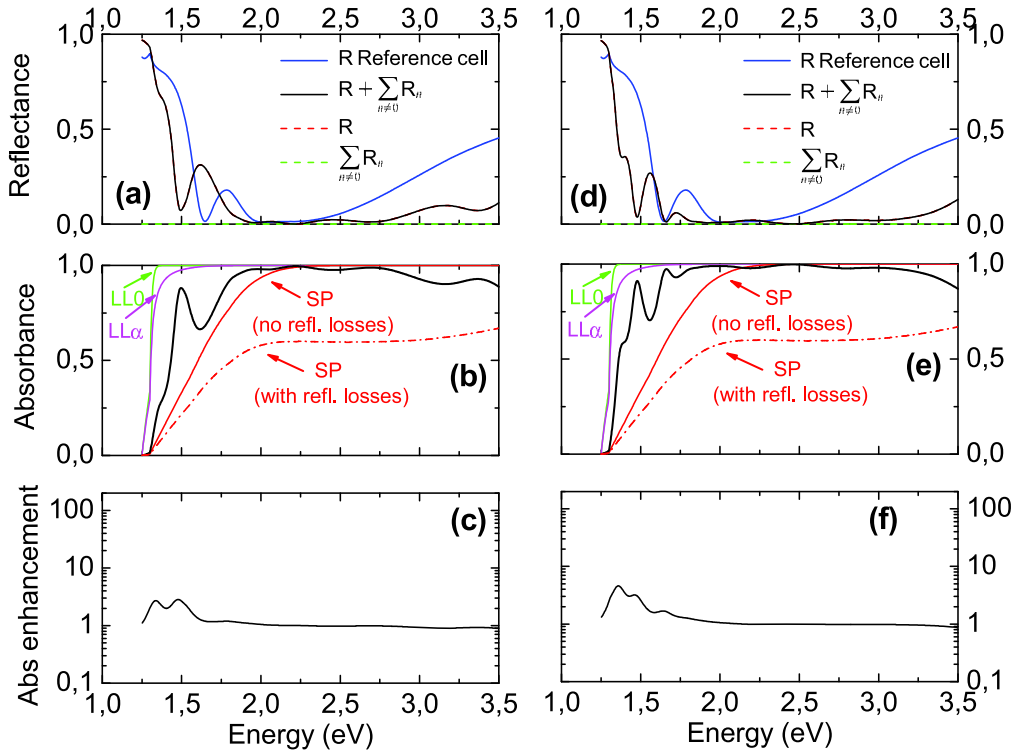

Fig. 9. Calculated optical spectra (for unpolarized light) for a-Si PV cells patterned with optimal 1D simple lattice (d=300 nm, a=300 nm, h=210 nm, b/a=0.55): reflectance $R_{n=0}$ and contributions from diffraction in air $\sum_{n\neq 0} R_n$ (**a**), absorbance A (**b**) and absorption enhancement with respect to single pass absorption without reflection losses, F (**c**). Calculated optical spectra (for unpolarized light) for a-Si PV cells patterned with optimal 2D square lattice (d=300 nm, a=300 nm, h=215 nm, b/a=0.4): reflectance $R_{n=0}$ and contributions from diffraction in air $\sum_{n\neq 0} R_n$ (**d**), absorbance A (**e**) and absorption enhancement with respect to single pass absorption without reflection losses, F (**f**). For absorption the Lambertian limits LL0 and LLα are reported, together with single-pass absorption with and without reflection losses.

#156735 - $15.00 USD Received 18 Oct 2011; revised 7 Dec 2011; accepted 8 Dec 2011; published 30 Jan 2012

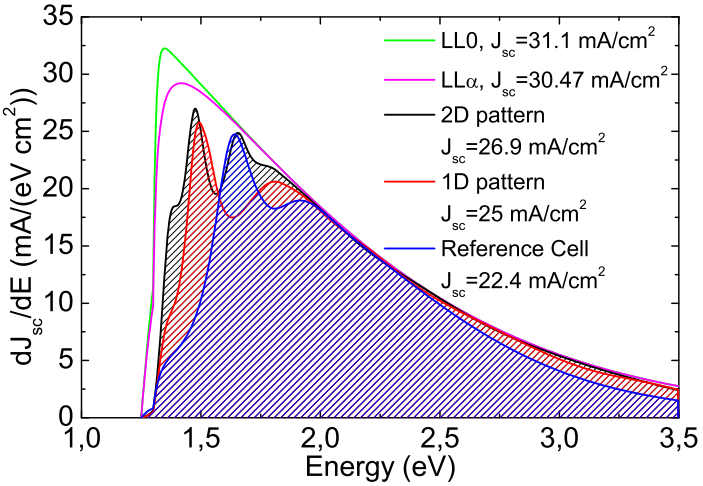

Fig. 10. Spectral contributions dJ_{sc}/dE to short-circuit current density J_{sc} for a-Si PV cells patterned with optimized 1D and square 2D lattices. The thickness d=300 nm, the optimal period a=300 nm.

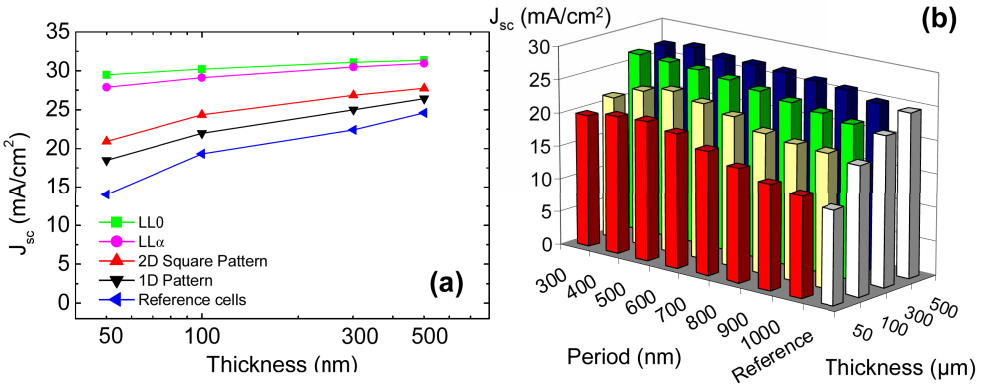

Fig. 11. **(a)** Calculated short-circuit current densities J_{sc} for a-Si PV cells patterned with optimized 1D and square 2D lattices varying the thickness d of the starting active material's slab. **(b)** J_{sc} for optimal configurations as a function of period a and thickness d.

#156735 - $15.00 USD Received 18 Oct 2011; revised 7 Dec 2011; accepted 8 Dec 2011; published 30 Jan 2012

these effects depends on the cell structure and on the spectral range. We showed that patterned cells give higher absorption and higher J_{sc} with respect to planar reference cells. This is mainly due to light trapping that increases absorption in the low energy region where the intrinsic absorption is weak, and to the broadband reduction of reflection losses, that is achieved by the intermediate photonic pattern, whose effective refractive index is intermediate between that of the AR coating and that of silicon. In particular, 2D patterns perform always better than 1D ones, thanks to improved diffraction properties into the quasi-guided modes of the structure. It is important to remark that diffraction and anti-reflection properties of a given photonic structure are intimately related and cannot be considered separately.

The final goal is to find structures that approach the limit of a Lambertian light scatterer. In this respect the present results show that there is still much room for improvement. From the comparison with Lambertian light trapping limits (especially the LLα limit, which is generally valid in the case of arbitrary absorption) we conclude that the J_{sc} generated by the investigated structures is intermediate between the calculated values for the planar reference cells (with AR coating and back reflector) and the ultimate limits. Two main guidelines can be derived for the future design of more efficiency thin film cells with a photonic pattern:

- reflection losses have to be reduced over the largest possible spectral range,
- light trapping has to be tailored to increase absorption at low energy, without promoting additional diffraction in air.

The key point, and also the main difficulty, is that this optimization has to be performed over the full solar spectral range to give further, relevant J_{sc} increase.

In terms of reduction of reflection losses, the front pattern could be improved towards a multilevel pattern, for example with lattices of rods or pillars with gradually varying radius etched on the front surface. This would give a smoother variation of effective refractive index from air to the active material, that is the basic concept for high efficiency AR coating design. Since the pattern would be periodic, diffraction inside the structure and, hence, light trapping would be performed. In terms of more efficient light trapping schemes, multiple photonic patterns (perhaps subdivided between front and back surfaces) could also increase the efficiency compared to a single pattern. This multiple pattern approach could also be generalized for multi-junction PV cells, where each junction in the stack could be patterned with a photonic lattice whose period has to be tuned depending on the absorption threshold of the active material.

However we expect that on ordered structure alone will not allow reaching the Lambertian limits for light trapping over the full solar spectrum. Indeed, the broad range of Fourier components needed for light scattering suggests that some amount of disorder has to be added. The combination of ordered structures like those considered in this work, together with microroughness on a sub-wavelength scale, appears to be especially promising as it would take advantage of optimized diffraction in the optical range as well as Rayleigh scattering with a continuous spectrum of wavevector components. The role of quasi-guided resonances in such a situation is well worth investigating.

In this work we have not considered electrical transport and the possible presence of defects at the patterned surfaces, giving rise to surface recombination. While electronic transport in the active material could benefit from reduced layer thicknesses when the Lambertian limit is approached, the issue of surface recombination in a patterned structure could be a crucial one. A high-efficiency ultra-thin film PV cell is likely to require careful optimization of light management, electronic transport, and surface passivation, just like for conventional bulk silicon solar cells.

#156735 - $15.00 USD Received 18 Oct 2011; revised 7 Dec 2011; accepted 8 Dec 2011; published 30 Jan 2012

Acknowledgments

We are grateful to Simone Zanotto for partecipating in the early phase of this work, and to Alex Mellor for helpful suggestions. This work was supported by Fondazione Cariplo under project 2010-0523 ”Nanophotonics for thin-film photovoltaics”, and by the EU through Marie Curie Action FP7-PEOPLE-2010-ITN project no. 264687 ”PROPHET”.

#156735 - $15.00 USD Received 18 Oct 2011; revised 7 Dec 2011; accepted 8 Dec 2011; published 30 Jan 2012